

Study of a Tm:Ho:YLF laser pumped by a Raman shifted erbium-doped fibre laser at 1678 nm

Yu.L. Kalachev, V.A. Mikhailov, V.V. Podreshetnikov, I.A. Shcherbakov

Abstract. The lasing, spectral, and luminescent characteristics of a Tm:Ho:YLF laser pumped by a Raman shifted erbium-doped fibre laser ($\lambda = 1678$ nm) into the 1682-nm absorption line of the ${}^3\text{H}_6 \rightarrow {}^3\text{F}_4$ transition of the Tm^{3+} ion are studied. It is shown that the total (with respect to the absorbed power) and slope laser efficiencies upon pulsed pumping reach 46% and 50%, respectively. The output radiation power in the cw regime is 400 mW. The comparative measurements showed that pumping by a fibre laser at 1678 nm is more efficient than diode pumping at 792 nm.

Keywords: laser, Tm, Ho, YLF, laser diode, fibre-laser pumping.

1. Introduction

Two-micron lasers with diode pumping into the Tm^{3+} absorption line in the region of 800 nm, which are based on YLF, YAG, YAP, and other crystals doped either only with Tm^{3+} or with Tm^{3+} and Ho^{3+} ions, are well studied and widely used in various fields of science, engineering, and medicine [1, 2].

It is of considerable interest to increase the efficiency and output power and to improve the beam quality of these lasers. One of the promising methods in this direction is the choice of the most efficient wavelength for laser pumping. Laser pumping of Tm:Ho:YLF active elements (AEs) into the ${}^3\text{H}_6 \rightarrow {}^3\text{F}_4$ absorption line of the Tm^{3+} ion at $\lambda = 1682$ nm was previously proposed and realised in [3–5]. As a pump source, the authors of [4, 5] used a home-made cryogenic frequency-tuneable CO:MgF₂ laser pumped by a neodymium laser at $\lambda = 1.34$ μm . However, the use of nitrogen-cooled pump lasers restricts the field of application of such devices. In addition, the power of this pump source is low.

In the present work, we propose for the first time to pump a Tm:Ho:YLF laser by an erbium fibre laser with SRS frequency conversion operating at a fixed wavelength of 1678 nm, which well coincides with the peak of the ${}^3\text{H}_6 \rightarrow {}^3\text{F}_4$ absorption band of the Tm ion.

The positive features of Raman shifted fibre lasers (RFLs) as laser pump sources are the high power and stability of the output radiation, as well as the nearly perfect spatial characteristics owing to the single-mode regime of their operation.

Fibre lasers are compact, reliable, and emit polarised radiation, which is an important advantage in some cases. The RFL pumping leads to smaller Stokes losses in AEs compared to the pumping by laser diodes (LDs) even when the quantum yield of cross-relaxation from the ${}^3\text{H}_4$ level is two. Our experiments showed that these advantages of RFL pumping considerably extend the potentialities of experimental investigations of Tm:Ho:YLF laser generation and accompanying processes, in particular, up-conversion [3, 6–8].

According to the energy level diagram of the Tm:Ho:YLF crystal [9, 10] (Fig. 1), LD pumping at 792 nm (arrow 792) populates the upper laser level ${}^5\text{I}_7$ of the Ho ion via the energy transfer from the ${}^3\text{F}_4$ level of the Tm ion (arrow 4), which, in turn, is populated as a result of the cross-relaxation processes ${}^3\text{H}_4 \rightarrow {}^3\text{F}_4$, ${}^3\text{H}_6 \rightarrow {}^3\text{F}_4$ (arrows 1). The cross relaxation occurs with a noticeable efficiency at the Tm concentration above 2% [11]. At the Tm concentration of 5%, the quantum yield of the cross-relaxation exceeds 1.8%, which ensures a high

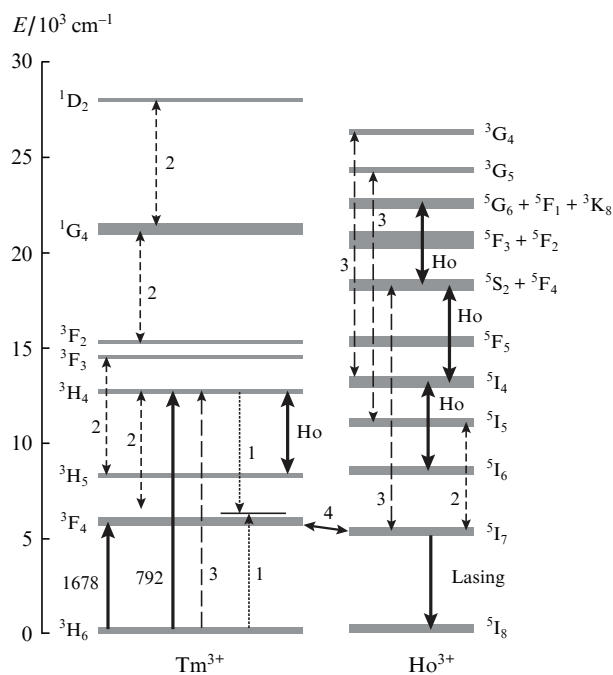


Figure 1. Energy level diagram of Tm^{3+} and Ho^{3+} ions in YLF. The arrows indicate LD pumping at a wavelength of 792 nm (792), fibre-laser pumping at 1678 nm (1678), cross-relaxation (1), transitions that are quasi-resonant with the RFL radiation (2), transitions that are quasi-resonant with the LD radiation (3), Tm–Ho energy transfer (4), transitions induced by intracavity laser photons (Ho).

Yu.L. Kalachev, V.A. Mikhailov, V.V. Podreshetnikov, I.A. Shcherbakov A.M. Prokhorov General Physics Institute, Russian Academy of Sciences, ul. Vavilova 38, 119991 Moscow, Russia; e-mail: kalachev@kapella.gpi.ru, mikhailov@kapella.gpi.ru, director@gpi.ru

Received 10 December 2009; revision received 1 March 2010
Kvantovaya Elektronika 40 (4) 296–300 (2010)
Translated by M.N. Basieva

efficiency of Tm:Ho:YLF lasers. However, these high concentrations lead to a high heat dissipation density in the AE, which can deteriorate the output beam quality due to a strong thermal lens. To use smaller concentrations of Tm, it is necessary to study the efficiency of Tm:Ho:YLF lasers operating under direct pumping of the 3F_4 level (arrow 1678), when the cross-relaxation is not directly involved.

2. Experimental conditions

The laser scheme is shown in Fig. 2. As active element (4), we used a Tm:Ho:YLF crystal $\varnothing 10 \times 2$ mm in size cut so that its geometric axis was perpendicular to the crystallographic axis c . The concentrations of Tm and Ho ions in the YLF crystal were 5% and 0.5%, respectively. According to [4], the LD-pumped Tm:Ho:YLF laser has the maximum efficiency at this ion concentration ratio. The plane-parallel faces of the AE were not antireflection coated. The AEs were pumped by a single-mode RFL (ELR-3-1680M, IRE-Polyus). The wavelength and linewidth of the pump laser radiation were 1678 and 2.4 nm, respectively. The output power was varied within 3 W. The pump beam was focused into the AE by objective (2). The output power was varied within 3 W. The pump beam was focused into the AE by objective (2). Pumping at a wavelength of 792 nm was performed using a fibre-coupled diode array (LIMO); the numerical aperture, the fibre diameter, and the maximum cw output power were 0.22, 200 μm , and 20 W, respectively.

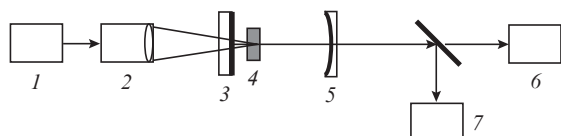


Figure 2. Scheme of the experimental setup:

(1) fibre-coupled pump laser; (2) focusing objective; (3) dichroic input mirror; (4) active element; (5) output coupler; (6) power meter; (7) MDR-204 monochromator.

The laser cavity used in the experiments was formed by plane dichroic mirror (3), which was transparent for the pump radiation and highly reflecting in the spectral region of 2 μm , and spherical output coupler (5) with a curvature radius of 52 mm and a reflection coefficient at the laser wavelength of 98% or 95%. To optimise the laser characteristics, it was possible to vary the cavity length within a range of 4–52 mm. The pump radiation was coupled into the cavity through dichroic mirror (3) with transmittances of $\sim 95\%$ at a wavelength of 1678 nm and 90% at 792 nm.

3. Spectral characteristics

The absorption spectra were recorded using a Shimadzu UV-3600 spectrophotometer with an error of 0.5 nm, and the luminescence spectra were measured using an MDR-204 monochromator (LOMO-Photonics) (error 1.4 nm in the case of a 1200-mm^{-1} grating, resolution 0.03 nm). Figure 3 shows the absorption and oscillation spectra of the Tm:Ho:YLF active element upon pumping by an RFL. The oscillation spectrum has a typical shape and consists of several narrow lines with different intensities in the vicinity of 2.05 μm . The intensity ratio of the oscillation spectrum components insignificantly changed with changing the experimental conditions.

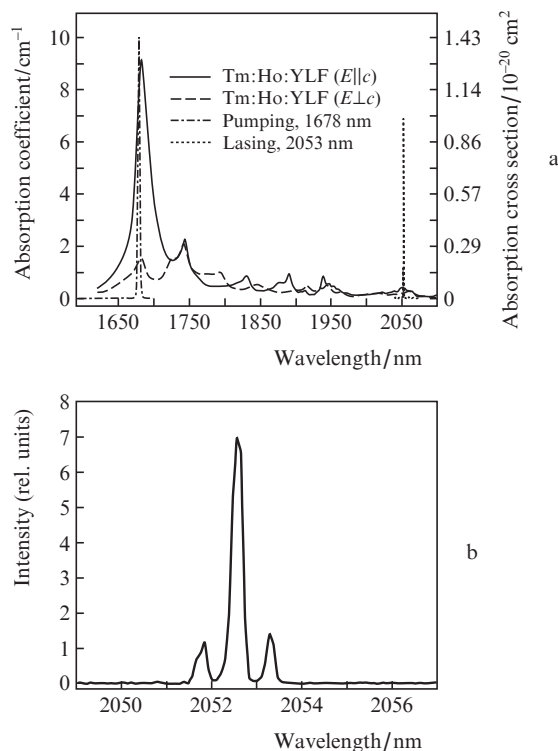


Figure 3. Absorption (a) and lasing (b) spectra of a 2-mm-thick Tm:Ho:YLF crystal.

These specific features of the oscillation spectrum were also retained in the case of LD pumping.

4. Optimisation of experimental conditions

One of the advantages of pumping by a single-mode fibre laser compared to diode pumping is the possibility of focusing the pump beam into the AE to a spot with a considerably smaller diameter, which allows one to achieve a higher pump intensity and to form long thin waists in lasers with extended active media. In our experiments, the diameter of the fibre pump laser spot was varied from 14 to 150 μm .

The laser characteristics were studied as functions of the pump power absorbed in the AE. We prefer to determine the lasing efficiency as a function of the absorbed rather than, as is frequently done, of the incident pump power, because the fraction of the pump power absorbed in the AE is not constant and decreases with increasing the pump power density (Fig. 4). The absorption of pump radiation in the AE decreases approximately by 20% as the pump power increases

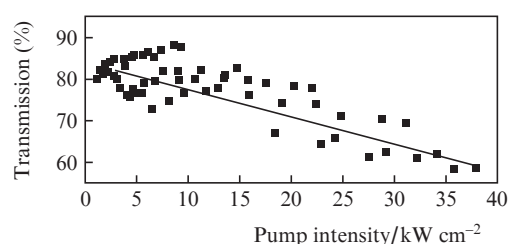


Figure 4. Absorption of pump radiation in the AE versus the pump intensity.

to 40 kW cm^{-2} . The partial decrease in the absorption of the active medium is caused by the partial equalisation of the populations of the absorption band levels under action of the pump field. In addition, a decrease in the absorption coefficient is caused by increasing temperature of the crystal [7]. The absorbed pump power was measured in the process of two-micron lasing, and the temperature dependence of the absorption coefficient was measured in a thermostat placed into the Shimadzu UV-3600 spectrophotometer.

Figure 5a shows the variations in the absorption line spectrum observed as the crystal temperature increases in the range of $25\text{--}147^\circ\text{C}$, which is characteristic of the pumped regions of solid-state lasers with longitudinal diode pumping. One can see that, as the temperature increases within this region, the absorption at the pump wavelength 1678 nm decreases by approximately 10% (Fig. 5b), which is quite substantial and comprises almost half the change in the absorption shown in Fig. 4. The decrease in the active medium absorption with temperature was taken into account when estimating the laser efficiency.

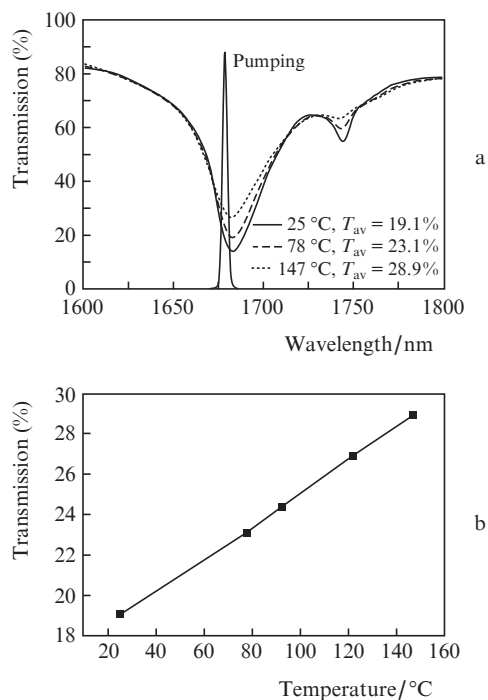


Figure 5. Transmission spectra T_{av} of a 2-mm-thick Tm:Ho:YLF active element ($E||c$) at different temperatures (a) and temperature dependence of the AE transmission at the pump wavelength (b).

The lasing efficiency of the Tm:Ho:YLF laser was studied at different pump spot diameters in the cavities 50 and 4 mm long (Figs 6a, b). The experiments showed that, under our conditions, the lasing efficiency for a rather long cavity (50 mm) slightly depends on the pump spot diameter (Fig. 6a).

The experimental points in Figs 6–9 correspond to the laser radiation power averaged over a series of independent measurements. The error in the average values does not exceed 5% with the measurement error in the series below 15%.

In the short cavity, the pump spot diameter affects the laser output power much stronger than in the long cavity. This can be most clearly seen in the dependence of lasing efficiency on the pump spot diameter (Fig. 7).

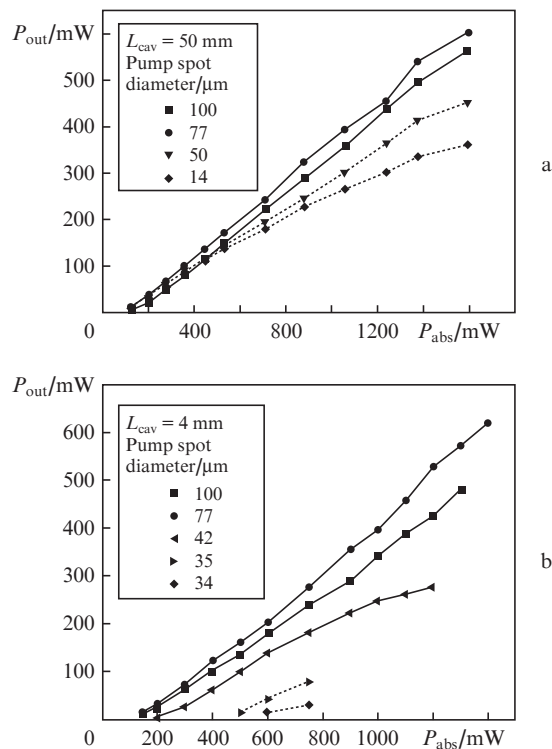


Figure 6. Dependences of the laser output power in the case of cavities 50 (a) and 4 mm (b) long on the pump power absorbed in the AE at different pump spot diameters.

One can see a pronounced flat maximum in the region of 60–90- μm diameters. The laser efficiency smoothly decreases at larger pump spot diameters, which well agrees with increasing laser threshold. However, the main distinguishing feature of the short cavity is the existence of a region of small diameters at which even a small (by 2–3 μm) decrease in the pump spot diameter strongly decreases the laser efficiency up to the complete termination of lasing. In particular, at an absorbed pump power of 600 mW and focal spot diameters below 40 μm , lasing under our conditions does not occur at all. Such a strong decrease in the efficiency can be related to the effect of a very imperfect thermal lens induced in the AE under our conditions, whose characteristic transverse dimensions are considerably smaller than the diameter of the fundamental

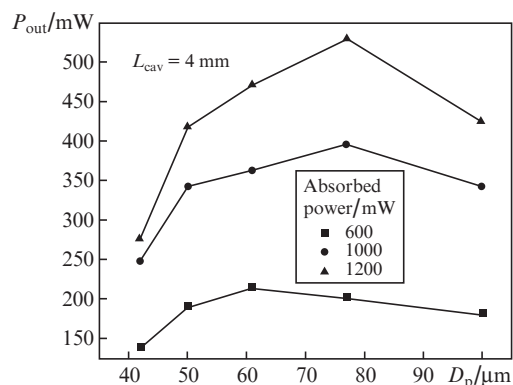


Figure 7. Dependences of the output power of the laser with a 4-mm-long cavity on the pump spot diameter at different values of the absorbed pump power.

transverse cavity mode. Probably, some contribution to the efficiency reduction is made by the up-conversion processes, which, being more intense in the region of high pump power densities, decrease the population of the upper laser level and lead to additional heat release.

The highest lasing efficiency was achieved in the 4-mm-long cavity (Fig. 8). A slightly lower efficiency was observed for the 50-mm-long cavity, which is close to the cavity stability boundary. Lasers with intermediate cavity lengths also had a lower efficiency.

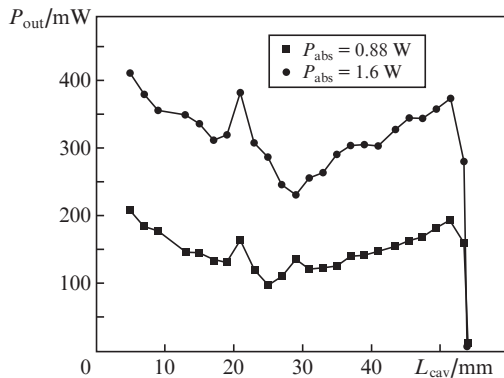


Figure 8. Dependences of the laser output power on the cavity length at the absorbed pump power of 0.88 and 1.6 W.

5. Laser characteristics

The output characteristics of a Tm:Ho:YLF laser with the 5-mm-long cavity under pumping by a RFL are shown in Fig. 9. The AE holder was kept at room temperature. The pump spot diameter ($\sim 75 \mu\text{m}$) was optimum according to the curves in Fig. 7. The output mirror reflectance was 95%. The maximum lasing efficiency and output power in the cw regime were limited by the thermal breakdown of the AE and reached $\sim 40\%$ and 400 mW, respectively. The slope efficiency in this case was 44%. Higher slope and total efficiencies ($\sim 50\%$ and 46%, respectively, at a peak power of 630 mW) were achieved in the case of pulsed pumping with a factor of 1:4 and a pulse duration of 100 μs . The laser output power in the pulsed regime was limited by the maximum allowable power of the RFL.

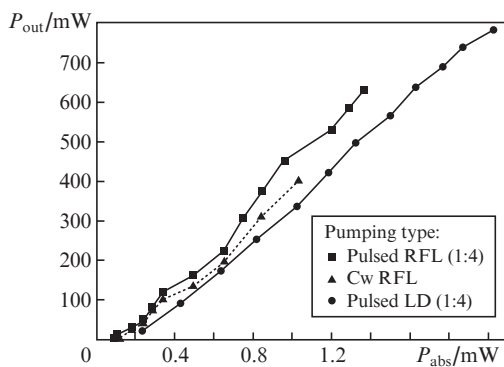


Figure 9. Dependences of the laser power on the absorbed pump power in the cw and pulsed (off-duty factor 1.4) regimes under diode and fibre pumping.

For comparison, we performed experiments using diode pumping under the same conditions. The LD beam was focused into the AE to a spot 160 μm in diameter. The slope and total laser efficiencies reached 42% and 36%, respectively, at the peak output power up to 780 mW (Fig. 9). Comparing the efficiencies obtained under RFL and LD pumping, one can see that they are higher in the first case.

Thus, it is experimentally shown that the direct pumping of the ${}^3\text{H}_6\text{--}{}^3\text{F}_4$ transition of Tm ions by the fibre laser followed by the excitation transfer to the ${}^5\text{I}_7$ level of Ho ions is more efficient than the pumping at 792 nm, when the ${}^3\text{F}_4$ level is populated as a result of cross-relaxation [11]. Note that this result was obtained in the case of a high ($\sim 5\%$) concentration of Tm ions. At the same time, in the case of a low ($\sim 1\%$) concentration of Tm ions, one can use longer AEs, which are easier cooled and, hence, can operate with a higher average output power. Under these conditions, pumping directly into the ${}^3\text{H}_6\text{--}{}^3\text{F}_4$ line will be even more advantageous compared to diode pumping. To form a long pump channel 80–100 μm in diameter will be not a difficult problem.

6. Up-conversion processes

The energy level diagram shown in Fig. 1 demonstrates numerous processes populating the high-lying levels of Tm and Ho. In addition to the light-induced transitions (arrows 2 and 3), an important role is also played by interactions of excited ions (for example, summation of excitations), namely, of Tm ions at the ${}^3\text{F}_4$ level with Ho ions at the ${}^5\text{I}_7$ level (${}^3\text{F}_4\text{--}{}^3\text{H}_6$, ${}^5\text{I}_7\text{--}{}^5\text{I}_5$) and of excited Ho ions with each other (${}^5\text{I}_7\text{--}{}^5\text{I}_8$, ${}^5\text{I}_7\text{--}{}^5\text{I}_6$), as well as by other interactions that lead to the population of high-lying excited states [6, 7, 12, 13]. In the case of diode pumping (arrows 3), the resonance transitions in Ho are ${}^5\text{I}_7\text{--}{}^5\text{S}_2 + {}^5\text{F}_4$, ${}^5\text{I}_5\text{--}{}^3\text{G}_5$, ${}^5\text{I}_4\text{--}{}^3\text{G}_4$. The strong laser radiation field in the cavity partially equalises the populations of levels involved into transitions resonant with the laser frequency. These transitions are denoted by arrows Ho in Fig. 1: the ${}^5\text{I}_6\text{--}{}^5\text{I}_4$, ${}^5\text{I}_4\text{--}{}^5\text{S}_2 + {}^5\text{F}_4$, ${}^5\text{S}_2 + {}^5\text{F}_4\text{--}{}^5\text{G}_6 + {}^5\text{F}_1 + {}^3\text{K}_8$ transitions of Ho ions and the ${}^3\text{H}_5\text{--}{}^3\text{H}_4$ transitions of Tm ions. In the case of pumping by a fibre laser (arrows 2), the resonance transition is ${}^5\text{I}_7\text{--}{}^5\text{I}_5$ in Ho^{3+} ions, while the ${}^3\text{F}_4\text{--}{}^3\text{H}_4$, ${}^3\text{H}_5\text{--}{}^3\text{F}_3$, ${}^3\text{F}_3\text{--}{}^1\text{G}_4$, and ${}^1\text{G}_4\text{--}{}^1\text{D}_2$ transitions of Tm ions are nearly resonance. The effect of the laser field remains the same as in the case of the diode pumping. Thus, in both cases, due to the up-conversion processes, the AEs efficiently luminesce in the visible and

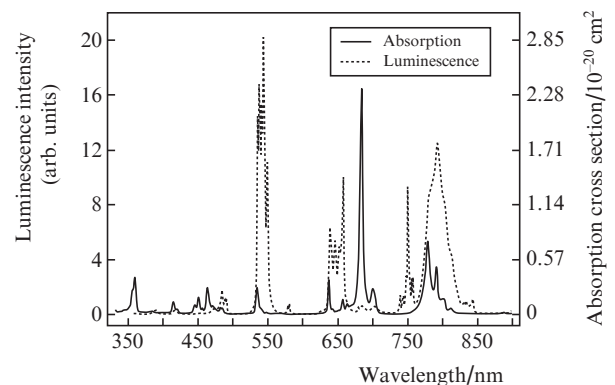


Figure 10. Absorption and luminescence spectra of a Tm:Ho:YLF crystal upon RFL pumping.

near-IR regions. For the considered laser, the up-conversion transitions are unfavourable because they decrease the population of the upper laser level and cause excessive heating of the AE, thus decreasing the lasing efficiency.

The luminescence spectrum upon RFL pumping measured in the absence of lasing is shown in Fig. 10. The most intense is the wide line in the region of 0.8 μm (the dominance of this line is not pronounced in Fig. 10 due to a low sensitivity of the used PMT at wavelengths above 0.7 μm).

A similar luminescence spectrum was also observed upon diode pumping, but the 0.8- μm line in this case was completely overridden by the high-power pump radiation. The green luminescence line (~ 550 nm) looks noticeably brighter in the case of RFL than of diode pumping.

7. Conclusions

A Raman shifted erbium-doped fibre laser operating at a wavelength of 1678 nm is proposed and studied as a source for pumping a Tm:Ho:YLF laser into the $^3\text{H}_6$ – $^3\text{F}_4$ absorption line of the Tm $^{3+}$ ion (peaked at 1682 nm). The experiments showed that the pumping by a RFL causes more efficient

lasing than the conventional diode pumping into the 792-nm line of the $^3\text{H}_6$ – $^3\text{H}_4$ transition. Taking into account the high power, high beam quality, stability, and reliability of the fibre laser in combination with its commercial availability, we can conclude that this laser source is promising for pumping efficient high-power lasers based on Tm-doped AEs, namely, on Tm:Ho:YLF, Tm:Ho:YAP, Tm:YLF, Tm:YAP.

The total and slope laser efficiencies of the Tm:Ho:YLF laser pumped by a RFL in the cw regime reach 40% and 44%, respectively, at the output power up to 400 mW, which, under our experimental conditions, is limited by the AE breakdown due to thermoelastic deformations caused by the pump radiation. Under pulsed pumping with a factor of 1:4, i.e., at a lower thermal load on the AE, the total and slope efficiencies increase to 46% and 50%, respectively. This testifies to the potential possibility of increasing these efficiencies in the cw regime. The diode pumping at the wavelength 792 nm is noticeably less efficient.

A natural continuation of this work is the study of Tm:Ho:YLF lasers with low ($\sim 1\%$) concentrations of Tm ions from the viewpoint of their efficiency and output beam quality.

Acknowledgements. The authors thank V.A. Smirnov for useful discussions. This work was supported by the program ‘Fundamental Problems of Photonics and Physics of New Optical Materials’ of the Department of Physical Sciences of RAS.

References

1. Kohei M., Toshikazu I., Shoken I., Masahiko S., Tetsuo A., Kazuhiro A., Atsushi S. *J. Nat. Inst. Information and Communications Techn.*, **51** (1/2), 167 (2004).
2. Jean B., Bende T., *Solid-State Mid-Infrared Laser Sources* (Berlin: Springer, 2008) Vol. 89, p. 530.
3. Payne S.A., Smith L.K., Kway W.L., Tassano J.B., Krupke W.F. *J. Phys.: Condens. Matter*, **4**, 8525 (1992).
4. Cornaccia F., Di Lieto A., Marony P., Minguzzi P., Toncelli A., Tonelli M., Sorokin E., Sorokina I. *Appl. Phys. B*, **73**, 191 (2001).
5. Baronti B., Cornaccia F., Di Lieto A., Marony P., Toncelli A., Tonelli M. *Optics and Lasers in Engineering*, **39**, 277 (2003).

6. Kucks S., Sokolska I. *Chem. Phys. Lett.*, **325**, 257 (2000).
7. Rustad G., Stenersen K. *IEEE J. Quantum Electron*, **32** (9), 1645 (1996).
8. Hehlen M.P., Kuditcher A., Lenef A.L., Ni H., Shu Q., Rand S.C., Rai J., Rai S. *Phys. Rev. B*, **61**, 1116 (2000).
9. Janssen H.P., Linz A., Leavitt R.P., Morrison C.A., Wortman D.E. *Phys. Rev. B*, **11**, 92 (1975).
10. Walsh B.M., Barnes N.P., Di Bartolo B. *J. Appl. Phys.*, **83** (5), 2772 (1998).
11. So S., Mackenzie J.J., Shepherd D.P., Clarkson W.A., Betterton J.G., Gorton E.K. *Appl. Phys. B*, **84**, 389 (2006).
12. Ozen G., Salihoglu S. *Opt. Commun.*, **180**, 323 (2000).
13. Danilov A.A., Zubenko D.A., Kalitin S.P., Nasel'skii S.P., Noginov M.A., Ostroumov V.G., Privis Yu.S., Rustamov I.R., Saidov Z.S., Semenov S.G., Smirnov V.A., Shcherbakov I.A. *Trudy IOFAN*, **26**, 5 (1990).